



Myrtle Essential Oil-Loaded Alginate Nanoparticles: A Dual Therapeutic Approach for Cytotoxicity Against Skin Cancer Cells and Antibacterial Effects on Common Pathogens

Hamid Moradi¹ , Mojdeh Safari² , Razieh Ranjbar³ , Karrar S. Zayed⁴ , Mahmoud Osanloo⁵

1. Student Research Committee, Fasa University of Medical Sciences, Fasa, Iran

2. Finetech in Medicine Research Center, School of Medicine, Iran University of Medical Sciences, Tehran, Iran

3. Department of Medical Biotechnology, School of Advanced Technologies in Medicine, Fasa University of Medical Sciences, Fasa, Iran

4. Department of Laboratory Investigations, Faculty of Science, University of Kufa, Najaf, Iraq

5. Department of Medical Nanotechnology, School of Advanced Technologies in Medicine, Fasa University of Medical Sciences, Fasa, Iran

Article Info

Article Type:

Research Article

Article history:

Received

23 Mar 2024

Received in revised form

18 Apr 2024

Accepted

18 May 2024

Published online

14 Jun 2024

Publisher

Fasa University of
Medical Sciences

Abstract

Background & Objectives: The skin, being the body's largest organ, is not only susceptible to one of the most prevalent forms of cancer but also vulnerable to a myriad of pathogens, including bacteria. Myrtle essential oil (EO) has been shown to possess both anticancer and antimicrobial properties. This study aimed to investigate the efficacy of alginate nanoparticles containing myrtle EO on melanoma (A375) and epidermoid carcinoma (A431) cell lines, as well as on some common bacteria, including *Escherichia coli*, *Pseudomonas aeruginosa*, and *Staphylococcus aureus*.

Materials & Methods: Initially, myrtle EO was analyzed using Gas Chromatography-Mass Spectrometry. Subsequently, alginate nanoparticles were prepared via the ionic-gelation method and characterized by dynamic light scattering, Zeta potential, and attenuated total reflectance-Fourier transform infrared spectroscopy. Encapsulation efficacy was then determined using UV-Vis spectrometry. Both cytotoxicity assessment (MTT assay) and evaluation of antibacterial effects (microdilution assays) were conducted using the 96-well plate format.

Results: The major compounds identified in myrtle EO were α -pinene, 1,8-cineole, linalool, linalool acetate, and geranyl acetate. The alginate nanoparticles exhibited a size of 160 ± 9 nm, a SPAN of 0.96, and a Zeta potential of -26 ± 2 mV. The encapsulation efficacy was determined to be 78.4%. It was found that the nanoparticles demonstrated cytotoxicity against A375 and A431 cells with IC₅₀ values of 211 μ g/mL and 308 μ g/mL, respectively. The most potent antibacterial effect was observed against *S. aureus* (IC₅₀: 266 μ g/mL).

Conclusion: The alginate nanoparticles containing myrtle EO, which exhibited notable cytotoxicity against melanoma and epidermoid carcinoma cells as well as potent antibacterial effects, show promise for further investigation *in vivo* studies.

Keywords: Nanotechnology; Complementary Medicine; Cytotoxicity; Melanoma

Cite this article: Moradi H, Safari M, Ranjbar R, Zayed K.S, Osanloo M. Myrtle Essential Oil-Loaded Alginate Nanoparticles: A Dual Therapeutic Approach for Cytotoxicity Against Skin Cancer Cells and Antibacterial Effects on Common Pathogens. *J Adv Biomed Sci.* 2024; 14(3): 177-189.

DOI: 10.18502/jabs.v14i3.16355

Corresponding Author: Mahmoud Osanloo,
Department of Medical Nanotechnology, School of
Advanced Technologies in Medicine, Fasa University
of Medical Sciences, Fasa, Iran.
Email: osanloo_mahmood@yahoo.com



Introduction

Cancer remains the second leading cause of mortality among individuals under 85 years of age in the United States. As per the latest



2024 cancer statistics released by the American Cancer Society, it is projected that the number of individuals afflicted with this condition will surpass 2 million (1, 2). The skin, which constitutes approximately one-sixth of the total body weight, is not only the body's largest organ but also the site of the fifth most common cancer type, non-melanoma skin cancer (3, 4). Melanoma, a malignant transformation of melanocytes, accounts for about 75% of skin cancer-related deaths (5, 6). It is anticipated that 99,700 new cases of cutaneous melanoma will be diagnosed in 2024 (1, 2).

In the present study, two human cancer cell lines were employed: A375, a melanoma cell line, and A431, an epidermoid carcinoma cell line (7, 8). Both cell lines are widely utilized in research to elucidate cancer biology and evaluate the efficacy of various treatments and drugs on cancer (9). Furthermore, the skin's extensive surface area renders it particularly susceptible to damage from physical and chemical agents, as well as various pathogens such as bacteria. Among these, *Escherichia coli* (gram-negative), *Pseudomonas aeruginosa* (gram-negative), and *Staphylococcus aureus* (gram-positive) are three common opportunistic pathogens capable of inducing pain, swelling, and severe skin infections (10-12).

The primary challenges in cancer treatment can be attributed to the heterogeneous nature of cancer, multidrug resistance, adverse effects of therapeutic agents, cancer recurrence, and metastasis (13). While antibiotic therapy remains the first line of defense against bacterial infections, concerns regarding antibiotic resistance continue to mount (14, 15). In this context, essential oils (EO) and extracts derived from medicinal plants represent valuable resources for developing novel therapeutic agents (16, 17). For instance, *Myrtus communis*, or common myrtle (Family: Myrtaceae), exhibits a diverse array of biological activities, including antioxidant, anticancer, antidiabetic, antibacterial, and



antifungal properties (18, 19). The antibacterial efficacy of myrtle EO has been confirmed against a broad spectrum of bacteria, including *Parvimonas micra* (gram-positive strain) and *Aggregatibacter actinomycetemcomitans* (gram-negative strain) (20).

Despite the advantages of medicinal plants, such as their lack of resistance, safety profile, and cost-effectiveness, there remains a need to enhance their efficiency. Nanoparticles offer a promising approach to augment the efficiency and stability of these natural compounds by modifying the physical and chemical properties of their cargoes, such as EOs or extracts (21, 22). Among these, alginate nanoparticles have garnered significant attention in drug delivery systems due to their non-toxicity, biodegradability, and biocompatibility (23, 24). The present study marks the first report of alginate nanoparticles containing myrtle EO. We investigated their anticancer and antibacterial effects against two cell lines, A375 and A431, and three bacterial strains, *S. aureus*, *E. coli*, and *P. aeruginosa*.

Materials and Methods

Alginate sodium and calcium chloride were procured from Sigma-Aldrich (USA). EO extracted from *Myrtus communis* leaves was obtained from Tabib Daru Company (Iran). A375 (CRL-1619) human malignant melanoma cells and A431 (CRL-1555) human epidermoid carcinoma cells, as well as *E. coli* (ATCC 25922), *P. aeruginosa* (ATCC 27853), and *S. aureus* (ATCC 25923), were sourced from the Pasteur Institute of Iran.

Identification of Compounds of Myrtle EO Using Gas Chromatography-Mass Spectrometry (GC-MS) analysis

The analysis of myrtle EO was conducted using a gas chromatography apparatus (Agilent 6890, HP-5MS column, USA) coupled with a mass spectrometer (Agilent 5973, USA), adhering to the procedures outlined in our prior study (25).



In brief, the column temperature program commenced at 40 °C (maintained for 1 minute), then increased at a rate of 3 °C per minute until reaching 250 °C, where it was held for 60 minutes. Both the injection port and detector temperatures were set at 250 °C and 230 °C, respectively. Additional operational parameters included the use of helium (99.999%) as the carrier gas, with a split flow of 25 mL/min, septum purge of 6 mL/min, and a column flow rate of 1 mL/min. Mass spectra were acquired in full scan mode within the 50–550 m/z range, utilizing an ionization energy of 70 eV. Retention indices were computed using a mixture of n-alkanes (C6–C27) based on the Van den Dool and Kratz (1963) formula (26). The identification of EO components involved a combination of temperature-programmed retention indices and mass spectra, which were compared with data from ADAMS and NIST 17 (27, 28). Relative abundances were determined through peak area normalization.

Preparation and Characterizations of Alginate Nanoparticles Containing Myrtle EO

The nanoparticles were prepared using the ionic-gelation method, as detailed in our previous investigation (29). Initially, myrtle EO (0.25% w/w) and tween 20 (0.2% w/w) were blended on a stirrer at 1000 rpm for 3 minutes. Subsequently, an aqueous alginate solution (0.25% w/w) was gradually added and stirred for approximately 3 minutes. Following this, aqueous calcium chloride solutions (1.40, 1.00, 0.06, and 0.02% w/w) were added dropwise (separately) and stirred for 40 minutes to stabilize. The mean size of the resulting alginate nanoparticles containing myrtle EO was

determined using a dynamic light scattering (DLS) device (k-One, Nano, Ltd, Korea), which provided information on nanoparticle size distribution (SPAN). Particle size below 200 nm and a SPAN less than 1 were considered the desired size characteristics. A sample (No. 3 in Table 1) meeting these criteria was selected for further characterization and biological assays. As a negative control group, alginate nanoparticles (Alg(-EO)) were prepared using the same method and ingredients as the chosen sample, but without the addition of myrtle EO.

Furthermore, Attenuated Total Reflectance-Fourier Transform InfraRed (ATR-FTIR) spectroscopy (Bruker, Tensor II, Germany) was conducted to identify the chemical characteristics of the sodium alginate, myrtle EO, Alg(-EO), and alginate nanoparticles containing myrtle EO. This analysis was performed at room temperature in the wavenumber range of 500–3500 cm⁻¹. ATR-FTIR spectroscopy has also been proposed to evaluate possible interactions between alginate nanoparticles and myrtle EO, qualitatively confirming the loading of the EO in nanoparticles. In addition, UV-Vis spectrometry was employed to determine the encapsulation efficacy of myrtle EO in alginate nanoparticles. To construct the standard concentration-absorption curve, various concentrations (5–200 µg/mL) of myrtle EO were dissolved in absolute ethanol. Subsequently, its absorption in the 190–450 nm wavelength range was scanned, and the highest common wavelength across all concentrations was selected as the λ_{max} . The linear regression equation of concentration versus absorption was then calculated using Excel software.

Table 1. Ingredients and size analyses of prepared alginate nanoparticles containing Myrtle EO

Sample	Myrtle EO (% w/w)	Alginate solution (% w/w)	Tween 20 (% w/w)	Calcium Chloride (% w/w)	Particle Size	SPAN
1	0.25	0.25	0.20	0.14	480	1.56
2	0.25	0.25	0.20	0.10	241	0.99
3	0.25	0.25	0.20	0.06	160	0.96
4	0.25	0.25	0.20	0.02	225	1.23



Given that the R² value exceeded 95%, the accuracy of this regression was confirmed.

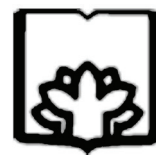
To determine the EO's encapsulation efficacy, the alginate nanoparticles containing myrtle EO were subjected to centrifugation at 10,000 rpm for 30 minutes at 4°C. Subsequently, the amount of myrtle EO in the supernatant was calculated by applying its absorption value to the obtained regression equation. The encapsulation efficiency was then calculated using the following formula: (initial EO – EO in supernatant) / initial EO × 100.

Investigation of Cytotoxic Effects of Alginate Nanoparticles Containing Myrtle EO

The cytotoxic impact of the sample (alginate nanoparticles containing myrtle EO) on A375 and A431 cells was assessed using the MTT assay. The cells were cultured in Dulbecco's Modified Eagle Medium (DMEM) perfect medium, supplemented with 10% FBS and 1% antibiotics, with 10⁴ cells/well seeded in 96-well plates. Following a 24-hour incubation at 37°C and 5% CO₂ until 80% confluence was achieved, the medium was replaced with 50 µL/well of fresh DMEM perfect medium and serial dilutions of the sample (dissolved in phosphate buffered saline (PBS) at concentrations ranging from 39-1250 µg/mL). Concurrently, PBS solution and Alg(-EO) were added to control and negative control groups, respectively, in lieu of serial dilutions. After a 24-hour incubation period, the medium was substituted with 50 µL/well of MTT solution (0.5 mg/mL in DMEM). Following a 4-hour incubation, 100 µL/well of dimethyl sulfoxide was added to dissolve the formazan crystals. Cell viability was then determined by calculating the ratio of the optical density of samples to that of the control at 570 nm using a plate reader (Synergy HTX Multi-Mode Reader, USA).

Investigation of Antibacterial Effects of Alginate Nanoparticles Containing Myrtle EO

The antibacterial efficacy of the sample against *E. coli*, *P. aeruginosa*, and *S. aureus* was evaluated using the microdilution method in a 96-well plate format. Suspended bacterial colonies



in Muller-Hinton broth with 0.5 McFarland turbidity (1.5×10^8 CFU/mL) were combined with serial dilutions of the sample (dissolved in PBS at concentrations ranging from 39-1250 µg/mL) in the wells (50:50 µL/well). Concurrently, 50 µL/well of PBS solution and Alg(-EO) were introduced to the plates as control and negative control groups, respectively, in place of serial dilutions. Following a 24-hour incubation period, bacterial growth was quantified by calculating the ratio of the optical density of the samples to that of the control at 630 nm using a plate reader.

Statistical Analyses

The experiments were conducted in triplicate, with results presented as mean and standard deviation. Two-way ANOVA was employed to analyze the results of cellular toxicity and antibacterial effects of alginate nanoparticles containing myrtle EO at different concentrations against the aforementioned cells and bacteria. Analyses and graph plotting were performed using GraphPad Prism software. Additionally, the IC₅₀ values for the samples were computed using CalcuSyn software (free version, BIOSOFT, UK).

Results

The identified compounds in myrtle EO are listed in Table 2. The major compounds were found to be α-pinene (29.77%), 1,8-cineole (25.83%), linalool (9.16%), linalool acetate (5.94%), and geranyl acetate (3.40%).

The ingredients and size analyses of the prepared alginate nanoparticles containing myrtle EO are summarized in Table 1. Among the prepared samples, only the size characteristics of sample 2 met the acceptable criteria: particle size <200 nm and SPAN <1 (29). Consequently, this sample was selected for further investigation. Its DLS and Zeta potential profiles are illustrated in Figures 1A and 1B, respectively. The particle size, SPAN value, and Zeta potential were determined to be 160±9 nm, 0.96, and -26±2 mV, respectively.

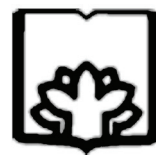


Table 2. Identified compound in myrtle EO using GC-MS analysis

Compound	Retention Index	Area	%
α -thujene	930	36284215	1.00
α -pinene	932	1070412470	29.77
carene	1002	93299232	2.59
3-carene	1008	39910111	1.11
1,8-cineole	1026	928574270	25.83
α -terpinene	1059	41028327	1.14
terpinolene	1088	47197833	1.31
linalool	1095	329363333	9.16
α -terpineol	1188	112704608	3.13
linalool acetate	1257	213802170	5.94
geranyl acetate	1381	122346095	3.40
<i>trans</i> -caryophyllene	1419	44454783	1.23
α -humulene	1438	41052490	1.14
viridiflorol	1592	58136977	1.61

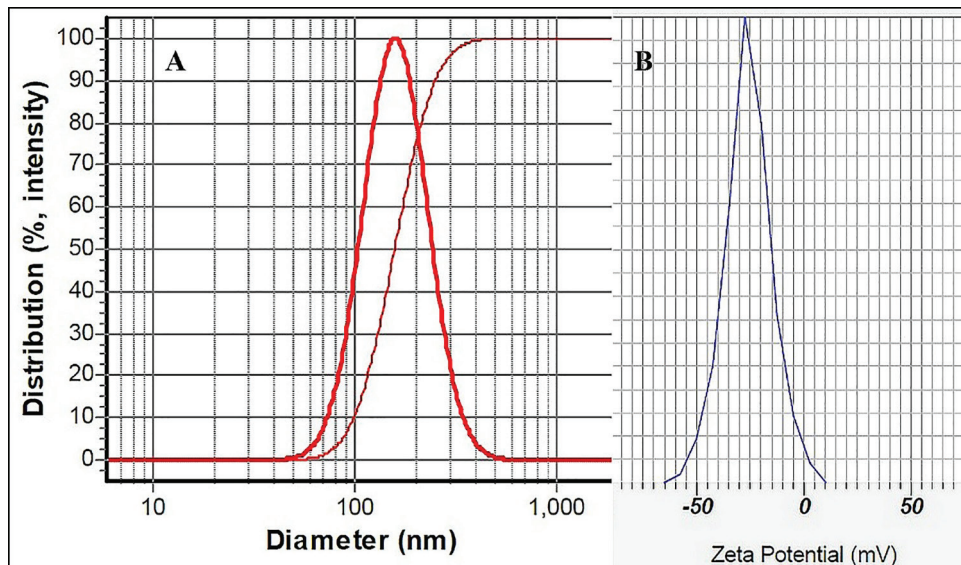


Figure 1. Size (A) and Zeta potential (B) profiles of alginate nanoparticles containing myrtle EO

ATR-FTIR spectra of sodium alginate, myrtle EO, Alg(-EO), and alginate nanoparticles containing myrtle EO are presented in Figure 2. The ATR-FTIR spectrum of sodium alginate (Figure 2A) exhibited characteristic absorption peaks corresponding to carboxylic acid (COOH), ether, and hydroxyl (OH) functional groups (30). Absorption peaks observed at 2838-2941 cm⁻¹ were attributed to stretching vibrations of aliphatic C-H bonds. A broad peak around 3246 cm⁻¹ was associated with hydroxyl

(-OH) groups in the sodium alginate structure. Characteristic peaks at 1596 and 1404 cm⁻¹ indicated asymmetric and symmetric stretching vibrations of carboxylate anions (-COO-), respectively. The absorption band at 1169 cm⁻¹ was attributed to C-O oscillation, whereas the peak at 1029 cm⁻¹ was linked to -COC- group oscillation (31). The ATR-FTIR spectrum of myrtle EO (Figure 2B) displayed a broad peak at 3468 cm⁻¹, corresponding to stretching vibrations of the hydroxyl (-OH) group (32, 33).

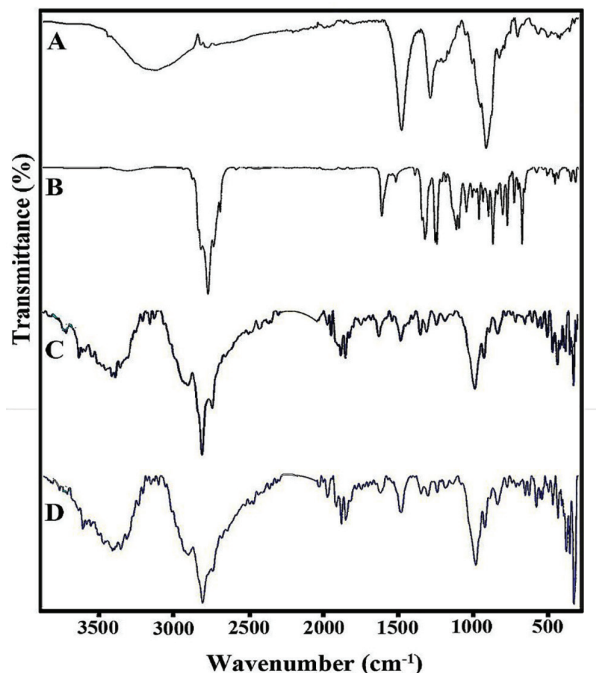


Figure 2. ATR-FTIR of A: sodium alginate, B: myrtle EO, C: alginate nanoparticles without EO (Alg(-EO)), and D: alginate nanoparticles containing myrtle EO

The band observed at 1234 cm⁻¹ was due to C–O asymmetric stretching in cyclic polyphenolic compounds, while the peak at 1364 cm⁻¹ was assigned to C–O stretching of the ester group. The band at 1445 cm⁻¹ was related to O–H bending vibrations, and the peak at 1644 cm⁻¹ was associated with C=C stretching vibrations. The characteristic peak at 1740 cm⁻¹ indicated C=O stretching vibrations. Bands at 2917 and 2966 cm⁻¹ were assigned to –CH symmetrical and asymmetrical stretch, respectively. The absorption peak at 2177 cm⁻¹ was related to C≡C stretching vibration, while bands at 1375 and 1053 cm⁻¹ were attributed to C–O stretch, indicating several oxygen-comprising functional groups in the myrtle EO structure.

The ATR-FTIR spectrum of Alg(-EO) (Figure 2C) revealed different absorption bands compared to that of sodium alginate (34). It comprised a broad peak around 3470 cm⁻¹, originating from the stretching vibration of hydroxyl groups, polymeric association, and intermolecular



hydrogen bonding (35). Peaks observed at 2924, 2855, and 1461 cm⁻¹ were assigned to asymmetric stretching of C–H, symmetric stretching of C–H, and bending vibrations of C–H, respectively. Bands at 1354, 1096, and 1034 cm⁻¹ were attributed to the secondary alcoholic group, stretching vibration of C–O–C in the pyranosyl ring, and stretching vibration of C–O. Peaks located at 489 and 576 cm⁻¹ were related to C–C skeletal vibrations and out-of-plane bending of C–H. Notably, the absorption region of O–H stretching vibration bands in Alg(-EO) was narrower than that of sodium alginate, due to the participation of OH and -COO groups of alginate in forming a chelating structure with calcium ions (Ca²⁺). Furthermore, the asymmetric stretching mode of the carboxylate ion in Alg(-EO) shifted to lower wave numbers compared to sodium alginate, as the replacement of Na⁺ with Ca²⁺ altered the radius, atomic weight, and charge density of the cation (36).

The presence of myrtle EO in the alginate nanoparticles was confirmed by ATR-FTIR analysis. In the spectrum of myrtle EO-loaded alginate nanoparticles (Figure 2D), characteristic bands of the individual components were recognized, albeit with some changes in peak position and intensity. This indicated an effective interaction between myrtle EO and alginate nanoparticles. Based on these ATR-FTIR results, it can be concluded that alginate nanoparticles hold promise as a carrier for myrtle EO in drug delivery systems (37).

The regression equation and calibration curve of myrtle EO, as obtained by UV-Vis spectrophotometry, are depicted in Chart 1. The encapsulation efficacy of myrtle EO in alginate nanoparticles was determined to be 78.4%.

The cytotoxic effects of alginate nanoparticles containing myrtle EO against A375 and A431 cells are summarized in Chart 2. A direct relationship was observed between the dose and the decrease in viability of both cell lines; however, Alg(-EO) did not affect cell viability.

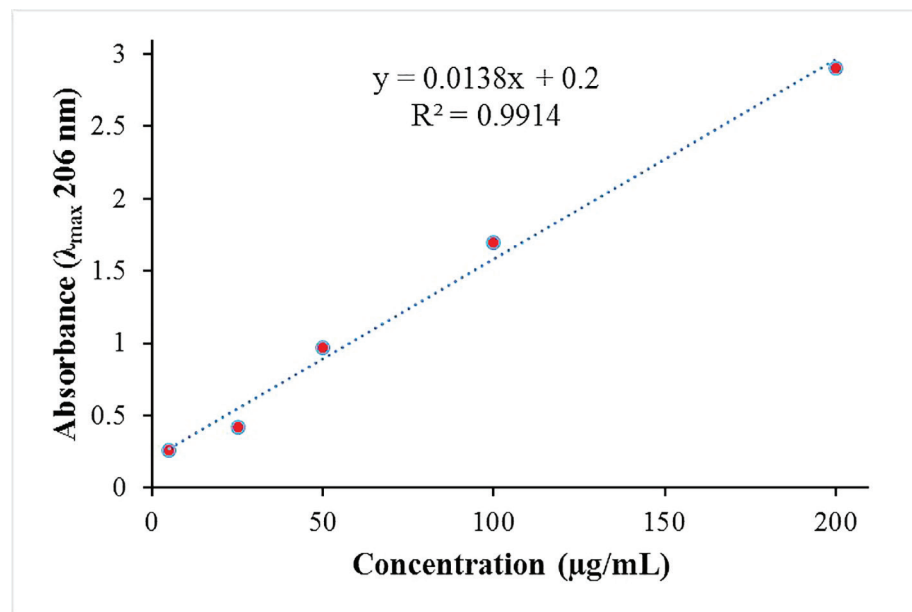


Chart 1. Linear regression equation and calibration curve of myrtle EO by UV-Vis spectrophotometer

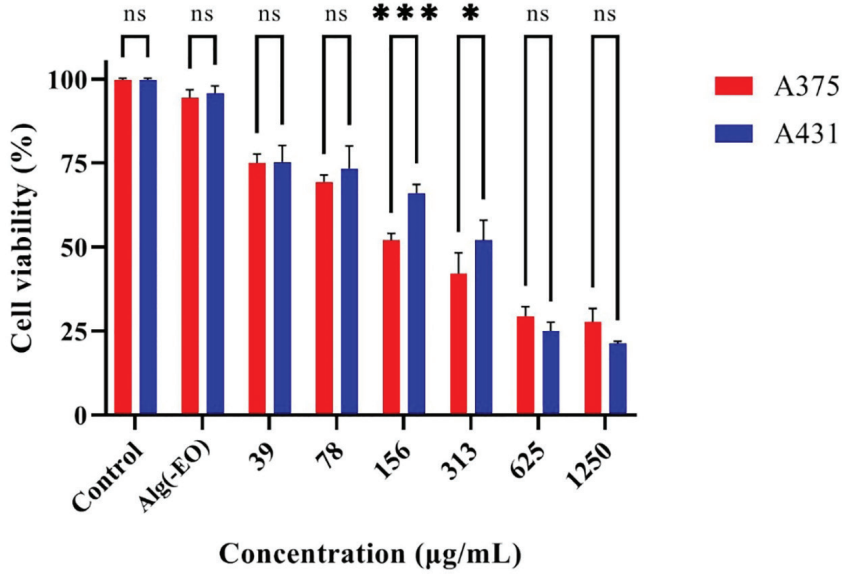


Chart 2. Cytotoxic effects of alginate nanoparticles containing myrtle EO. ns: not significant, ***: $P < 0.001$, and *: $P < 0.05$

The IC₅₀ values of the nanoparticles against A375 and A431 were calculated to be 211 (172-261) $\mu\text{g/mL}$ and 308 (192-492) $\mu\text{g/mL}$, respectively (Table 3).

The antibacterial effects of alginate nanoparticles containing myrtle EO are presented

in Chart 3. As the concentration increased, bacterial growth decreased. As shown in Table 1, the efficacy of nanoparticles against *S. aureus* was more potent, with an IC₅₀ value of 266 (165-429) $\mu\text{g/mL}$, compared to *E. coli* (614 (279-1351) $\mu\text{g/mL}$) and *P. aeruginosa* (478 (388-588) $\mu\text{g/mL}$).

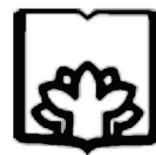


Table 3. Obtained IC_{50} values ($\mu\text{g/mL}$) of alginate nanoparticles containing myrtle EO

Factors	A375	A431	<i>E. coli</i>	<i>P. aeruginosa</i>	<i>S. aureus</i>
IC_{50}	211	308	614	478	266
LCL-UCL*	172-261	192-493	279-1351	388-588	165-429

*Lower and Upper Confidence Limits

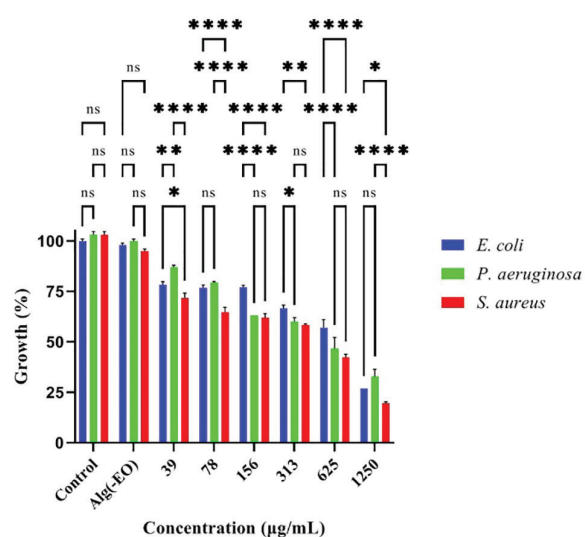


Chart 3. Antibacterial effects of alginate nanoparticles containing myrtle EO. ns: not significant, ****: $P < 0.0001$, **: $P < 0.01$, and *: $P < 0.05$

Discussions

The use of medicinal plants dates back to ancient civilizations, where indigenous communities relied on herbal medicines to maintain health and reduce diseases (38). With technological advancements, the mechanisms underlying the biological effects of medicinal plants have been gradually elucidated. For instance, the anti-cancer and antibacterial properties of myrtle EO have been well-established (18, 19), which formed the basis for its use in this study. Myrtle EO has been shown to induce apoptosis via various pathways, including the mitochondrial cytochrome c/Apaf-1/caspase-9 pathway, with the intrinsic pathway playing a more significant role than the extrinsic pathway (39). Furthermore, it has been observed that myrtle EO causes the loss of mitochondrial membrane potential, leading to the release of cytochrome c from mitochondria. Mitochondrial toxicity is considered a major indicator of cellular

deregulation due to the organelle's central role in cell cycle regulation, cell proliferation, and apoptosis induction (40).

Research has also demonstrated that myrtle EO can induce cell cycle arrest, particularly in the G1 phase. This effect impedes the proliferation of cancer cells by preventing their progression through the cell cycle, thereby limiting their growth and spread (41). Studies have shown the ability of myrtle extract to induce apoptosis in various cancer cell lines, including breast (MCF-7), liver (HepG2), cervical (HeLa), and colon (HCT116) cancer cells (25, 42). Notably, myrtle EO has been found to induce cell death through multiple mechanisms, including the cleavage of poly (ADP-ribose) polymerase (PARP), activation of caspases-3, -8, and -9, DNA fragmentation, and release of nucleosomes (43). Moreover, myrtle EO exhibits significant antioxidant properties, which are crucial in its anticancer effects. These antioxidants can neutralize free radicals, preventing oxidative stress that can damage cellular components and DNA, potentially leading to cancer development (44).

Some studies suggest that myrtle EO possesses antiangiogenic activities. Angiogenesis, the formation of new blood vessels, is a critical process in tumor growth and metastasis. By inhibiting angiogenesis, myrtle EO may help to starve tumors of the nutrients and oxygen needed for their growth (45). In silico studies, such as molecular docking analyses, have identified interactions between compounds in myrtle EO, like α -pinene, and specific cancer-related proteins. For example, α -pinene has shown high antioxidant and anticancer activity against the testis-specific protein on the Y chromosome (TSPY), suggesting a molecular basis for its anticancer effects (46).



The mechanism of antibacterial effects of myrtle EO can be attributed to several factors, including a cascade of reactions affecting the entire bacterial cell; these characteristics stem from the multi-component nature of EOs (47). The primary mechanism of action of myrtle EO against various bacteria is its ability to disrupt bacterial cell membranes, resulting in an inhibitory effect on vital cellular functions (48). This membrane disruption can lead to the leakage of cell contents and subsequent cell death (43). Several researchers have indicated that myrtle EO is mechanistically more active against gram-positive bacteria, such as *S. aureus*, than gram-negative ones, such as *E. coli*, due to differences in bacterial cell membrane interactions. Myrtle EO can separate membrane lipids, thereby increasing bacterial membrane permeability (48, 49). The greater sensitivity of gram-positive bacteria compared to gram-negative bacteria is primarily due to the ease with which antibiotics can penetrate their cell walls. The thick peptidoglycan layer in gram-positive bacteria allows antibiotics to reach their target sites, such as the bacterial cytoplasm or cell membrane, more easily. Consequently, gram-positive bacteria tend to be more sensitive to various drugs (50).

One study found that aqueous myrtle extracts exhibited both antibacterial and anticandidal activities. Proteomic analysis of *E. coli* treated with myrtle extract revealed upregulation of 42 proteins and downregulation of 6 proteins, indicating that the extracts affected protein expression within the bacterial cells. Approximately 85% of the identified proteins were from the cytoplasm and 15% from the microbial cell walls, suggesting that the extracts could penetrate the cells. A higher percentage of expressed proteins was associated with enzymatic activity, implying that myrtle extract may disrupt normal cellular processes by affecting enzyme function (51). Another study suggested that sub-inhibitory concentrations of

myrtle leaf extracts could induce the production of free radicals in *S. aureus*, which could be a possible mechanism for its antibacterial action. This indicates that myrtle may exert oxidative stress on bacterial cells, leading to their damage or death (52).

The use of medicinal plant EOs is often limited by instability, poor solubility, and low bioavailability of their active compounds. To address these issues, researchers have turned to nanotechnology, particularly nanoencapsulation, as a promising approach to increase the therapeutic potential of medicinal plants (53). In this study, alginate nanoparticles were employed. Alginate, a natural seaweed extract, is a linear chain of sugar units (M and G) that dissolve in water. When exposed to calcium chloride, the free hydroxyl groups on this natural polymer's units interact electrostatically with calcium ions. This attraction causes the alginate chains to crosslink, forming a three-dimensional network and creating alginate nanoparticles (54, 55). The advantages of alginate nanoparticles in drug delivery include simple and cost-effective preparation methods, the ability to form stable complexes, and improved drug efficacy (56, 57).

Interestingly, alginate nanoparticles containing myrtle EO have not been previously reported. However, some reports on other nanoformulations containing myrtle EO have been published. For instance, alginate nanoemulsion coating containing myrtle EO has demonstrated proper antibacterial effects against *Listeria monocytogenes* (58). In another study by our team, a nanogel of myrtle EO was developed, and its biological effects against A375, *E. coli*, and *S. aureus* were investigated in comparison to non-formulated EO. Their respective IC₅₀ values were 133 & 580, 583 & 4547, and 548 & 394 µg/mL (25). The efficacy of alginate nanoparticles containing myrtle EO (in the current study) was more potent than non-formulated EO. However, the efficacy of the nanogel against A375 was more potent than in this study; as these cells are



skin-originated, it was probably related to higher viscosity and better interaction with cell walls.

Furthermore, the anticancer effect of alginate nanoparticles containing myrtle EO on the A375 cell line was superior to that on A431. EOs have demonstrated selective anticancer effects on various types of cancer. Recent research has focused on showing that EOs possess cancer cell-targeting capabilities. They have been found to act through multiple pathways and mechanisms involving apoptosis, cell cycle arrest, and inhibition of angiogenesis (59, 60). Additionally, the best antibacterial efficacy was obtained against a gram-positive bacterium (*S. aureus*) for the aforementioned reasons. This efficacy was comparable to or more potent than many available reports. For instance, the IC₅₀ value of nanoemulsion containing *Origanum majorana* EO was reported as 580 µg/mL (61), while IC₅₀ values of nanogel and nanoemulsion containing another EO were reported as 187 and 3732 µg/mL, respectively (62). Although the alginate nanoparticles introduced in the current study have shown promising anticancer and antibacterial properties, it is suggested that their efficacy needs further evaluations in animal models. Additionally, their efficacy against other cancer cells and bacteria could be investigated to broaden the scope of their potential applications.

Conclusion

Alginate nanoparticles containing myrtle EO exhibited significant cytotoxicity against melanoma (A375) and epidermoid carcinoma (A431) cells, with IC₅₀ values of 211 µg/mL and 308 µg/mL, respectively. Furthermore, potent antibacterial effects were observed, particularly against *S. aureus* (IC₅₀: 266 µg/mL). The encapsulation efficiency of myrtle EO in alginate nanoparticles was 78.4%. This research underscores the promising role of nanotechnology in enhancing the efficacy of medicinal plant EOs for potential applications in cancer treatment and bacterial infection



management.

Conflict of Interests

The authors declare no conflicts of interest.

Acknowledgement

Not applicable.

Ethics approval and Consent to Participate

This study received ethical approval. As the research did not involve human subjects, informed consent was not required.

Code of Ethics

IR.FUMS.REC.1402.089

Funding

This study was supported by a grant (No. 402097) from Fasa University of Medical Sciences.

Authors' Contributions

HM prepared the nanoparticles and drafted the manuscript in collaboration with MO. MS interpreted the ATR-FTIR data. RR conducted the antibacterial tests. MO designed the study, analyzed the data, performed the MTT assay, and contributed to drafting the manuscript. KSZ revised the manuscript. All authors contributed to the drafting and approval of the final manuscript.

References

- 1 Siegel RL, Giaquinto AN, Jemal A. Cancer statistics, 2024. CA Cancer J Clin. 2024;74(1):12-49.
- 2 Dizon DS, Kamal AH. Cancer statistics 2024: All hands on deck. CA Cancer J Clin. 2024;74(1):8-9.
- 3 Kanitakis J. Anatomy, histology and immunohistochemistry of normal human skin. Eur J Dermatol. 2002;12(4):390-401.
- 4 WHO. Cancer Key facts 2023 [cited 2023 Feb]. Available from: <https://www.who.int/news-room/fact-sheets/detail/cancer>.
- 5 Jänicke RU. MCF-7 breast carcinoma cells do not express caspase-3. Breast Cancer Res Treat. 2009;117:219-21.
- 6 Ranjbar R, Zarenezhad E, Abdollahi A, Nasrizadeh



M, Firoozian S, Namdar N, et al. Nanoemulsion and Nanogel Containing Cuminum cyminum L Essential Oil: Antioxidant, Anticancer, Antibacterial, and Antilarval Properties. *J Trop Med*. 2023;2023:5075581.

7 de Melo MRS, Ribeiro AB, Fernandes G, Squarisi IS, de Melo Junqueira M, Batista AA, et al. Ruthenium(II) complex with 2-mercaptopthiazoline ligand induces selective cytotoxicity involving DNA damage and apoptosis in melanoma cells. *J Biol Inorg Chem*. 2024;29: 159–168.

8 Nirmala JG, Akila S, Nadar MM, Narendhirakanan RT, Chatterjee S. Biosynthesized *Vitis vinifera* seed gold nanoparticles induce apoptotic cell death in A431 skin cancer cells. *RSC Advances*. 2016;6:82205-18.

9 Castagna A, Antonioli P, Astner H, Hamdan M, Righetti SC, Perego P, et al. A proteomic approach to cisplatin resistance in the cervix squamous cell carcinoma cell line A431. *Proteomics*. 2004;4(10):3246-67.

10 Abdollahi A, Zarenezhad E, Ghaznavi G, Khalili pour M, Osanloo M. Promising antibacterial activity of a mat of polycaprolactone nanofibers impregnated with a green nanogel. *Nanomed Res J*. 2020;5(2):192-201.

11 Lestari ES, Severin J, Filius P, Kuntaman K, Duerink D, Hadi U, et al. Antimicrobial resistance among commensal isolates of *Escherichia coli* and *Staphylococcus aureus* in the Indonesian population inside and outside hospitals. *Eur J Clin Microbiol Infect Dis*. 2008;27:45-51.

12 Esposito S, Ascione T, Pagliano P. Management of bacterial skin and skin structure infections with polymicrobial etiology. *Expert Rev Anti-infect*. 2019;17(1):17-25.

13 Yarian F, Yousefpoor Y, Hatami S, Zarenezhad E, Peisepar E, Alipanah H, et al. Comparison Effects of Alginate Nanoparticles Containing *Syzygium aromaticum* Essential Oil and Eugenol on Apoptotic Regulator Genes and Viability of A-375 and MCF-7 Cancer Cell Lines. *BioNanoScience*. 2023;13:911–9.

14 Fair RJ, Tor Y. Antibiotics and bacterial resistance in the 21st century. *Perspect Medicinal Chem*. 2014;6:25–64.

15 Reuter J, Merfort I, Schempp CM. Botanicals in dermatology: an evidence-based review. *Am J Clin Dermatol*. 2010;11:247-67.

16 Osanloo M, Ghaznavi G, Abdollahi A. Surveying the chemical composition and antibacterial activity of essential oils from selected medicinal plants against human pathogens. *Iran J Microbiol*. 2020;12(6):505-12.

17 Osanloo M, Yousefpoor Y, Alipanah H, Ghanbariasad A, Jalilvand M, Amani A. In-vitro Assessment of Essential Oils as Anticancer Therapeutic Agents: A Systematic Literature Review. *Jordan J Pharm Sci*. 2022;15(2):173-203.

18 Barhouchi B, Menacer R, Bouchkioua S, Mansour A, Belattar N. Compounds from myrtle flowers as antibacterial agents and SARS-CoV-2 inhibitors: In-vitro and molecular docking studies. *Arab J Chem*. 2023;16(8):104939.

19 Dhouibi I, Flamini G, Bouaziz M. Comparative Study on the Essential Oils Extracted from Tunisian Rosemary and Myrtle: Chemical Profiles, Quality, and Antimicrobial Activities. *ACS Omega*. 2023;8(7):6431-8.

20 Gursoy UK, Gursoy M, Gursoy OV, Cakmakci L, Koenonen E, Uitto V-J. Anti-biofilm properties of *Satureja hortensis* L. essential oil against periodontal pathogens. *Anaerobe*. 2009;15(4):164-7.

21 Sanei-Dehkordi A, Moemenbellah-Fard MD, Sereshti H, Shahriari-Namadi M, Zarenezhad E, Osanloo M. Chitosan nanoparticles containing *Elettaria cardamomum* and *Cinnamomum zeylanicum* essential oils; repellent and larvicidal effects against a malaria mosquito vector, and cytotoxic effects on a human skin normal cell line. *Chem Pap*. 2021;75:6545–56.

22 Gharpure S, Yadwade R, Chakraborty B, Makar R, Chavhan P, Kamble S, et al. Bioactive properties of ZnO nanoparticles synthesized using *Cocos nucifera* leaves. *3 Biotech*. 2022;12(2):45.

23 Wagle SR, Kovacevic B, Walker D, Ionescu CM, Shah U, Stojanovic G, et al. Alginate-based drug oral targeting using bio-micro/nano encapsulation technologies. *Expert Opin Drug Deliv*. 2020;17(10):1361-76.

24 WND DES, Attanayake AP, Arawwawala L, Karunaratne DN, Pamunuwa GK. In vitro antioxidant activity of alginate nanoparticles encapsulating the aqueous extract of *Coccinia grandis* L. *Turk J Chem*. 2023;47(4):715-25.

25 Roozitalab G, Yousefpoor Y, Abdollahi A, Safari M, Rasti F, Osanloo M. Antioxidative, anticancer, and antibacterial activities of a nanoemulsion-based gel containing *Myrtus communis* L. essential oil. *Chem Pap*. 2022;76(7):4261-71.

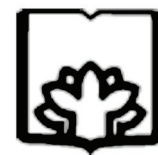
26 van Den Dool H, Dec. Kratz P. A generalization of the retention index system including linear temperature programmed gas—liquid partition chromatography. *J Chromatogr A*. 1963;11:463-71.

27 Adams RP. Identification of essential oil components



by gas chromatography/mass spectrometry: Allured publishing corporation Carol Stream, IL; 2007.

- 28 Standards NIO, Technology. Mass spectral library (NIST/EPA/NIH). National Institute of Standards and Technology Gaithersburg, MD; 2008.
- 29 Valizadeh A, Hosseinzadeh M, Heiran R, Hatami S, Hosseiniipour A, Osanloo M. Alginate nanoparticles containing *Lavandula angustifolia* essential oil as a potential potent, biocompatible and low-cost antitumor agent. *Polym Bull*. 2024;81:861–1874.
- 30 Kuczajowska-Zadrożna M, Filipkowska U, Józwiak T. Adsorption of Cu (II) and Cd (II) from aqueous solutions by chitosan immobilized in alginate beads. *J Environ Chem Eng*. 2020;8(4):103878.
- 31 Diep E, Schiffman JD. Encapsulating bacteria in alginate-based electrospun nanofibers. *Biomater Sci*. 2021;9(12):4364–73.
- 32 Modiri-Delshad T, Ramazani A, Khoobi M, Akbari Javar H, Akbari T, Amin M. Fabrication of chitosan/polycaprolactone/*Myrtus communis* L. extract nanofibrous mats with enhanced antibacterial activities. *Polym Polym Compos*. 2023;31:09673911231151506.
- 33 Ali Abuderman A, Syed R, A, Alyousef A, S, Alqahtani M, Shamsul Ola M, Malik A. Green synthesized silver Nanoparticles of *Myrtus communis* L (AgMC) extract inhibits cancer hallmarks via targeting aldose reductase (AR) and associated signaling network. *Processes*. 2019;7(11):860.
- 34 Thai H, Thuy Nguyen C, Thi Thach L, Thi Tran M, Duc Mai H, Thi Thu Nguyen T, et al. Characterization of chitosan/alginate/lovastatin nanoparticles and investigation of their toxic effects in vitro and in vivo. *Sci Rep*. 2020;10:909
- 35 Sarmento B, Ferreira D, Veiga F, Ribeiro A. Characterization of insulin-loaded alginate nanoparticles produced by ionotropic pre-gelation through DSC and FTIR studies. *Carbohydr Polym*. 2006;66(1):1–7.
- 36 Daemi H, Barikani M. Synthesis and characterization of calcium alginate nanoparticles, sodium homopolymannuronate salt and its calcium nanoparticles. *Sci Iran*. 2012;19(6):2023–8.
- 37 Sarei F, Dounighi NM, Zolfagharian H, Khaki P, Bidhendi SM. Alginate nanoparticles as a promising adjuvant and vaccine delivery system. *Indian J Pharm Sci*. 2013;75(4):442.
- 38 Les F, Cásedas G, López V. Bioactivity of Medicinal Plants and Extracts. *Biology (Basel)*. 2021;10(7):634.
- 39 Tretiakova I, Blaesius D, Maxia L, Wesselborg S, Schulze-Osthoff K, Cinatl J, et al. Myrtucomulone from *Myrtus communis* induces apoptosis in cancer cells via the mitochondrial pathway



involving caspase-9. *Apoptosis*. 2008;13(1):119–31.

- 40 Antico Arciuch VG, Elguero ME, Poderoso JJ, Carreras MC. Mitochondrial regulation of cell cycle and proliferation. *Antioxid Redox Signal*. 2012;16(10):1150–80.
- 41 Abdulqawi LNA, Quadri A, Islam S, Santra MK, Farooqui M. Chemical Compositions and Anticancer Activity of Yemeni Plant *Flemingia grahamiana* Wight & Arn. and *Myrtus communis* L. *Trop J Nat Prod Res*. 2021;5(5):877–82.
- 42 Guzelmeric E, Ugurlu P, Celik C, Sen NB, Helvacioğlu S, Charehsaz M, et al. *Myrtus communis* L. (Myrtle) plant parts: Comparative assessment of their chemical compositions, antioxidant, anticancer, and antimutagenic activities. *S Afr J Bot*. 2022;150:711–20.
- 43 Asgarpanah J, Ariamanesh A. Phytochemistry and pharmacological properties of *Myrtus communis* L. *Indian J Tradit Knowl*. 2015;14(1):82–7.
- 44 Ebrahimzadeh MA, Biparva P, Mohammadi H, Tavakoli S, Rafiei A, Kardan M, et al. Highly Concentrated Multifunctional Silver Nanoparticle Fabrication through Green Reduction of Silver Ions in Terms of Mechanics and Therapeutic Potentials. *Anticancer Agents Med Chem*. 2019;19(17):2140–53.
- 45 Dabbagh MM, Fadaei MS, Soleimani Roudi H, Baradaran Rahimi V, Askari VR. A review of the biological effects of *Myrtus communis*. *Physiol Rep*. 2023;11(14):e15770.
- 46 Fazeli Nasab B, Z Sayyed R, Sobhanizadeh A. In Silico Molecular Docking Analysis of α -Pinene: An Antioxidant and Anticancer Drug Obtained from *Myrtus communis*. *Int J Cancer Manag*. 2021;14(2):e89116.
- 47 Al-Maharik N, Jaradat N, Al-Hajj N, Jaber S. *M*yrtus communis L.: essential oil chemical composition, total phenols and flavonoids contents, antimicrobial, antioxidant, anticancer, and α -amylase inhibitory activity. *Chem Biol Technol Agric*. 2023;10(1):41.
- 48 Moura D, Vilela J, Saraiva S, Monteiro-Silva F, De Almeida JM, Saraiva C. Antimicrobial Effects and Antioxidant Activity of *Myrtus communis* L. Essential Oil in Beef Stored under Different Packaging Conditions. *Foods*. 2023;12(18):3390.
- 49 Caputo L, Capozzolo F, Amato G, De Feo V, Fratianni F, Vivenzio G, et al. Chemical composition, antibiofilm, cytotoxic, and anti-acetylcholinesterase activities of *Myrtus communis* L. leaves essential oil. *BMC complemet med ther*. 2022;22(1):142.
- 50 Silver LL. Challenges of antibacterial discovery. *Clin Microbiol Rev*. 2011;24(1):71–109.



51 Aabed K, Mohammed AE, Benabdulkamel H, Masood A, Alfadda AA, Alanazi IO, et al. Antimicrobial Mechanism and Identification of the Proteins Mediated by Extracts from Asphaltum punjabianum and Myrtus communis. *ACS Omega*. 2020;5(48):31019-35.

52 Najar AG, Mansouri S, Rahighi S. Effects of sub-inhibitory concentrations of *Myrtus communis* leave extracts on the induction of free radicals in *Staphylococcus aureus*; a possible mechanism for the antibacterial action. *Asian J Plant Sci*. 2009;8:551-6.

53 Bashir DJ, Manzoor S, Khan IA, Bashir M, Agarwal NB, Rastogi S, et al. Nanonization of Magnoflorine-Encapsulated Novel Chitosan-Collagen Nanocapsules for Neurodegenerative Diseases: In Vitro Evaluation. *ACS Omega*. 2022;7(8):6472-80.

54 Osanloo M, Ranjbar R, Zarenezhad E. Alginate Nanoparticles Containing Cuminum cyminum and Zataria multiflora Essential Oils with Promising Anticancer and Antibacterial Effects. *Int J Biomater*. 2024;2024:5556838.

55 Fernando IPS, Lee W, Han EJ, Ahn G. Alginate-based nanomaterials: Fabrication techniques, properties, and applications. *Chem Eng J*. 2020;391:123823.

56 George M, Abraham TE. Polyionic hydrocolloids for the intestinal delivery of protein drugs: alginate and chitosan—a review. *J Control Release*. 2006;114(1):1-14.

57 Ahmadi F, Saeedi M, Akbari J, Seyedabadi M, Ebrahimnejad P, Morteza-Semnani K, et al. Nano-hybrid Based on (Mn, Zn) Ferrite Nanoparticles Functionalized With Chitosan and Sodium Alginate for Loading of Curcumin Against Human Breast Cancer Cells. *AAPS PharmSciTech*. 2023;24(8):222.

58 Polat Yemis G, Sezer E, Sicramaz H. Inhibitory Effect of Sodium Alginate Nanoemulsion Coating Containing Myrtle Essential Oil (*Myrtus communis* L.) on *Listeria monocytogenes* in Kasar Cheese. *Molecules*. 2022;27(21): 7298.

59 Blowman K, Magalhaes M, Lemos MFL, Cabral C, Pires IM. Anticancer Properties of Essential Oils and Other Natural Products. *Evid Based Complement Alternat Med*. 2018;2018:3149362.

60 Gautam N, Mantha AK, Mittal S. Essential oils and their constituents as anticancer agents: a mechanistic view. *Biomed Res Int*. 2014;2014:154106.

61 Rasti F, Ahmadi E, Safari M, Abdollahi A, Satvati S, Ranjbar R, et al. Anticancer, antioxidant, and antibacterial effects of nanoemulsion of *Origanum majorana* essential oil. *Iran J Microbiol*. 2023;15(4): 565-573.

62 Alipanah H, Abdollahi A, Firooziyani S, Zarenezhad E, Jafari M, Osanloo M. Nanoemulsion and Nano-gel Containing *Eucalyptus globulus* Essential Oil; Larvicidal Activity and Antibacterial Properties. *Interdiscip Perspect Infect Dis*. 2022;2022:1616149.